4. M. F. Kazanskii, P. P. Lutsyk, and V. N. Oleinikov, Inzh.-Fiz. Zh., 3, No. 11 (1960).
5. F. M. Polonskaya, Zh. Tekh. Fiz., 23, No. 5 (1953).
6. V. D. Ermolenko, Inzh.-Fiz. Zh., 5, No. 10 (1962).
7. G. M. Kondrat'ev, Regular Thermal Conditions [in Russian], GITTL, Moscow (1954).
8. A. V. Lykov, Theory of Drying [in Russian], GÉI, Moscow (1950).
9. A. I. Chaplina, Inzh.-Fiz. Zh., 5, No. 9 (1962).
10. V. G. Kamenskii and V. P. Zhuravleva, Inzh.-Fiz. Zh., 25, No. 4 (1973).

A CALCULATION METHOD FOR TANGENTIAL SPRAY DRYERS

P. S. Kuts and V. A. Dolgushev

UDC 533.697:621.532

A method is presented for calculating the design parameters of a cylindrical spray dryer with tangential heat-carrier input; the relationships are analyzed.

Spiral flows of interacting phases are used in drying equipment because they set up a centrifugal pattern, which allows one to raise the concentration of the dispersed component, increase the relative speed of the phases, and thus accelerate the heat and mass transfer.

Here we examine a mathematical model for droplet interaction with a spiral gas flow in order to define the particle dynamics in relation to chamber design, with the object of providing basic concepts for design purposes.

The motion of a droplet in such a chamber is a complex curvilinear one in a spatial velocity distribution; the motion is affected by numerous different forces and other effects [1, 2]. The following external forces act on a particle in the general case: gravitation, reactive evaporation, molecular attraction, electrostatic, electromagnetic, and gasdynamic.

The latter includes the aerodynamic resistance, the counterpressure, the force due to turbulent mass transfer, and the Magnus force, the last arising by rotation of a particle around its axis.

It is impossible to reflect the combined action of all these forces fully in the differential equation, so various assumptions must be made.

We consider the motion of the heat carrier along a spiral line whose pitch is uniform along the length and radius, with the motion taken as stationary at an average velocity and as not involving rapid turbulent exchange. Radial leakage and secondary eddies are neglected, as is the loss of small particles toward the center of the chamber. It is assumed that the centrifugal force is purely radial, while the tangential and axial velocities of the particle and carrier are equal at each instant. In addition, we incorporate the change in droplet mass as well as the effects of the radial centrifugal force and viscous resistance.

The centrifugal force is defined by

$$F_{\text{c.f.}} = m_{\text{p}} \frac{w_{\text{p}}^2}{r} . \tag{1}$$

This force produces radial motion of the particle (separation speed), and the result is a resistance force exerted by the gas:

$$F_{\text{r.f.}} = \psi s \frac{(v - v_{\text{p}})^2 \gamma_1}{2q} , \tag{2}$$

A. V. Lykov Institute of Heat and Mass Transfer, Academy of Sciences of the Belorussian SSR, Minsk.
Translated from Inzhenerno-Fizicheskii Zhurnal, Vol. 30, No. 5, pp. 891-898, May, 1976. Original article submitted June 19, 1975.

where the aerodynamic-resistance coefficient [2] for $\mathrm{Re}_{(p)} \leq 1$ is $\psi = 24/\mathrm{Re}_{(p)}$, while for $\mathrm{Re}_{(p)} \leq 1000$ it is $\psi = [24/\mathrm{Re}_{(p)}](1 + 0.167\mathrm{Re}_{(p)}^{2/3})$.

The centrifugal force increases the relative velocity of the particle from zero up to some limiting value defined by $F_{c.f.} \leq F_{r.f.}$; equilibrium corresponds to Stokes' law, in which case the differential equation becomes

$$m_p \frac{w_p^2}{r} - \frac{24}{\mathrm{Re}_{(p)}} s \frac{(v - v_p)^2 \gamma_1}{2q} = m_p \frac{d(v - v_p)}{d\tau}, \tag{3}$$

where the first and second terms represent the centrifugal force and the viscous resistance, while the third is the inertial force in the radial direction.

The mass change in the evaporating droplet gives [3] $\delta^2 = \delta_0^2 - [(\delta_0^2 - \delta_c^2)/\tau_x]\tau$, which goes with the relations $m_p = \pi\delta^3\gamma_2/6q$, $s = \pi\delta^2/4$, and $\mathrm{Re}_{(p)} = \delta(v - v_p)/\nu$ to put (3) in the form

$$\frac{w_p^2}{r} - 18 \frac{\nu\gamma_1}{\left[\delta_0^2 - \left(\frac{\delta_0^2 - \delta_c^2}{\tau_x}\right)\tau\right]\gamma_2} (v - v_p) = \frac{d(v - v_p)}{d\tau}. \tag{4}$$

For convenience in integration, the relative velocity in the radial direction is put in the differential form $v - v_p = dr/d\tau$, while the coefficient to the first derivative for $\mathrm{Re}_{(p)} \leq 1$ is put as

$$A(\tau) = \frac{18\nu\gamma_1}{\left[\delta_0^2 - \left(\frac{\delta_0^2 - \delta_c^2}{\tau_x}\right)\tau\right]\gamma_2}, \tag{5}$$

and for $\mathrm{Re}_{(p)} \leq 1000$ as

$$A(\tau) = \frac{18\nu\gamma_1}{\left[\delta_0^2 - \left(\frac{\delta_0^2 - \delta_c^2}{\tau_x}\right)\tau\right]\gamma_2} (1 + 0.167\,\mathrm{Re}_{(p)}^{2/3}). \tag{6}$$

Then the general differential equation for a particle of variable mass moving in the radial direction becomes

$$\frac{d^2 r}{d\tau^2} + A(\tau)\frac{dr}{d\tau} - \omega^2 r = 0. \tag{7}$$

To determine the displacement of the particle together with the flow in the axial direction we need to know the pitch of the spiral motion, which is defined by

$$l_l = 2\pi r \,\mathrm{tg}\,\beta, \tag{8}$$

where β is the average angle represented by the spiral, which is related to the coefficient of angular-momentum conservation by

$$\mathrm{tg}\,\beta = \left(\frac{1}{\varepsilon_w^2} - 1\right)^{0.5}. \tag{9}$$

We assume a linear relationship between the axial component of the flow speed and the radius throughout the chamber, and also a relationship between the period of the rotational motion and time in terms of the angular velocity $\omega = \varepsilon_w w_{in}/R$ of the flow, in which the flow entrains the particle, which gives us the initial velocity axial direction as

$$u_{0p} = \omega r \left(\frac{1}{\varepsilon_w^2} - 1\right)^{0.5}.$$

We assume the motion to be uniformly decelerated and employ the condition that the axial component of the velocity becomes zero after a time τ_x on account of collision of jets with one another and with the end wall, which gives us the acceleration as

$$u_p' = -\left(\frac{1}{\varepsilon_w^2} - 1\right)^{0.5} \omega r/\tau_x,$$

and hence the particle velocity as

$$u_p = \omega r \left(\frac{1}{\varepsilon_w^2} - 1\right)^{0.5} (1 - \tau/\tau_x).$$

We integrate the latter expression to get the equation of motion for the particle in the axial direction as

$$x=\omega\left(\frac{1}{\varepsilon_w^2}-1\right)^{0.5}\int_0^{\tau} r\,(1-\tau/\tau_x)\,d\tau. \tag{10}$$

To analyze the drying in such a chamber in accordance with (7) and (10) we need to close the system of equations via additional relationships and also initial and boundary conditions. As an additional condition we specify the flow rate

$$w_{\text{in}}=\frac{Q}{\gamma_1\,(abk_a)\,3600} \tag{11}$$

and a formula relating the conservation of angular momentum to the geometrical and dynamic parameters:

$$\varepsilon_w=\frac{\left(1-\dfrac{k_a a}{2R}\right)}{1+0.027\mathrm{Re}_{(\text{in})}^{-0.25}\dfrac{2\pi RL}{abk_a}}\sqrt{1-\left(\frac{k_a a}{R\arccos\left(\dfrac{R-a}{R}\right)}\right)^2-\left(\frac{abk_a}{\pi(R^2-r_i^2)}\right)^2}, \tag{12}$$

together with the boundary conditions

$$\tau=0,\quad r=r_1,\quad \frac{dr}{d\tau}=0. \tag{13}$$

Equations (7) and (10)-(13) allow one to analyze the dynamic and design features, particularly any coupling between them. However, in calculating the chamber dimensions and sizes of components (particularly the inlet and outlet holes), we need to know the time required for a crust to form on a droplet, which defines the time at which the particle will no longer stick to the structure, and we also need to know the time required to dry to a given final water content.

The decisive factor in calculating the chamber radius is the time for crust formation, while the drying time is the relevant factor as regards the length. These times can be determined by experiment or from theory, but there are substantial difficulties in the calculation [4], so we have employed a method termed direct and inverse treatment.

In the first stage, we assume that the dimensions are known for a spray dryer or a particular output, together with the sizes of the inlet and outlet holes, the radius of the dispersal zone, and the dynamic parameters, but the crust-formation and drying times are unknown.

We substitute these quantities into (7) and (10) to derive the time τ_c for the particle to reach the outer radius of a chamber, and also the time τ_x spent by the particle in the chamber.

If an actual working plant shows no deposition, then τ_c may be taken as less than the time needed to reach the wall.

Also, τ_x (the drying time) can be judged from the quality of the final product, so one can calculate the nominal crust-formation and drying times on the basis of the entire set of definitive parameters for a particular mode of drying for a particular material.

In the second stage, we specify the productivity of the system as regards amount of water to be evaporated, the speed of the heat carrier in the tangential inlets, the same at the outlet, the loss of angular velocity, and the radius of the spraying zone, which gives us the coordinates of a particle at times τ_c and τ_x, which are related as follows to the dimensions of the chamber: the current radius of motion of an evaporating particle at time τ_c attains the chamber radius, while at time τ_x the coordinate in the axial direction attains the length.

We then solve the boundary-value problem represented by (7) and (10)-(13) to determine the sizes of the inlet holes; the formulation implies that the dimensions and the sizes of the holes are not unambiguously defined for a chamber of a given output, since all these are effected by the inlet speed. We thus have a relationship between the parameters of the motion of a droplet and the chamber design.

The actual hydrodynamics of the chamber and the details of the heat and mass transfer during drying are reflected in the bulk heat-transfer coefficient [4, 5], which may be derived by processing laboratory and production data for such spray dryers:

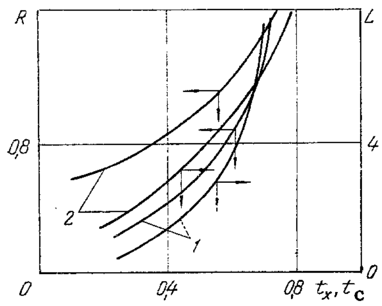

Fig. 1

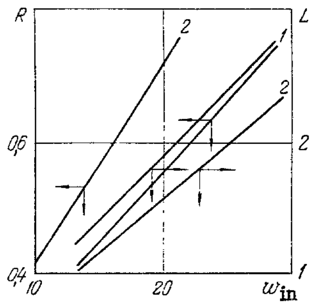

Fig. 2

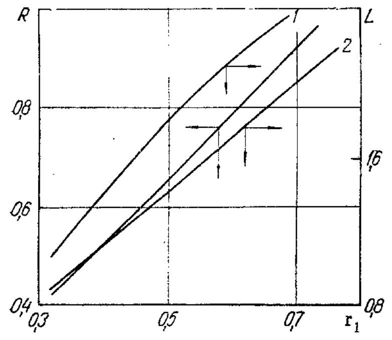

Fig. 3

Fig. 1. Drop coordinates in relation to τ_x and τ_c with $\tau_c = 0.6\,\tau_x$ for $\varepsilon_w = 0.5$; 1) $r_1 = 0.1$ m, $\omega = 17.2\ \mathrm{sec}^{-1}$; 2) $r_1 = 0.5$ m, $\omega = 14\ \mathrm{sec}^{-1}$. R, m; t_x and t_c, sec; L, m.

Fig. 2. Drop coordinates in relation to w_{in} for $r_1 = 0.1$ m, $\tau_c = 0.226$ sec, $\tau_x = 0.35$ sec; 1) $\varepsilon_w = 0.5$; 2) $\varepsilon_w = 0.7$. w_{in}, m/sec.

Fig. 3. Drop coordinates in relation to r_1 (in m) for $\tau_c = 0.226$ sec, $\tau_x = 0.35$ sec, $\omega = 10\ \mathrm{sec}^{-1}$, $\varepsilon_w = 0.5$ as derived from: 1) (10); 2) (10').

$$\alpha_v = 4.7\cdot 10^{-6}\,\frac{\lambda w_{(out)}^{1.5}}{\nu^{1.5}\,\delta_{3.2}^{0.5}}\,A_v^{-0.73}, \tag{14}$$

which applies with an error less than 12% within the following limits, $A_v^{-1} = 14$–47,

$$\delta_{3.2} = 25\cdot 10^{-6} - 65\cdot 10^{-6}\ \mathrm{m}, \qquad \mathrm{Re}_{(out)} = 4.5 - 32.$$

Equation (14) serves to close the boundary-value problem of (7) and (10)-(13), i.e., for specified working conditions, chamber size, and inlet hole size.

In formulating any calculation method, it is necessary to check the results for reliability, and in this connection we examine the rigor in the formulation.

When the system of (7) and (10)-(14) is being solved, errors of various origins can creep in; first, the initial data may not adequately describe the physical process on account of deficiencies in the theory and errors in the measurements. Secondly, errors arise in solving the equations themselves. As equations (7), (10), and (13) are familiar, the system was solved by a Minsk-32 computer, with the second-order differential equation of (7) integrated by the Runge–Kutta–Tanaka method with the standard RKTZ program, while transcendental equation (12) was solved by division of the intervals into halves, and the system as a whole was solved by steepest descent [6], in which case the calculations can be performed with any accuracy (in our case, the equations were solved with an error of 0.01), and so the errors arising from the second cause are unimportant. The basic error thus arises from inexact formulation of the problem.

It is sufficient to say that the empirical formula of (14) applies with a relative error of 12%; to estimate the possible errors in the formulation we thus assume that the pitch in the spiral motion is constant along the radius, in which case (10) becomes

$$x = \omega\left(\frac{1}{\varepsilon_\omega^2} - 1\right)^{0.5} R\tau\,(1 - 0.5\tau/\tau_x). \tag{10'}$$

Calculations from (10) and (10') show that a systematic error in determining the drying time of up to 29% arises from error in the formulation, as against only 14% for the chamber length. Therefore, one concludes, first of all, that the method is such that it tends to reduce the effects of error in determining the drying time on the accuracy of chamber size definition, while, secondly, that the calculation error is quite acceptable from the engineering viewpoint.

These relationships allow us to define the effect of the following factors on the chamber design: crust-formation and drying times (Fig. 1), input speed (Fig. 2), and sprayer design (Fig. 3).

Figure 1 shows that the chamber dimensions increase almost parabolically with the crust-formation time and, correspondingly, the drying time, with the result that the dimensions begin to increase rapidly beyond a certain point, which restricts the region of application of such plant.

TABLE 1. Sizes of Chamber and Inlet Holes in Relation to r_1 for $w = 10\ sec^{-1}$ and $k_a = 2$

r_1	w_{in}	R	L	a	b
0,668	14,5	0,873	1,91	0,143	0,398
0,680	14,8	0,889	1,95	0,144	0,389
0,692	15,1	0,904	1,98	0,144	0,382
0,704	15,3	0,920	2,02	0 144	0,375
0,716	15,6	0,936	2,05	0,144	0,369
0,728	15,9	0,951	2,08	0,144	0,364
0,740	16,1	0,967	2,12	0,243	0,359
0,752	16,4	0,983	2,15	0,143	0,354
0,764	16,6	0,998	2,19	0,142	0,351
0,776	16,9	1,01	2 22	0,141	0,348
0,788	17,2	1,03	2,26	0,139	0,346
0,800	17,4	1,05	2,29	0,138	0,345
0,812	17,7	1,06	2,33	0,136	0,344
0,824	17,9	1,08	2,36	0,134	0,344
0,836	18,2	1,09	2,39	0,132	0,345
0,848	18,5	1,11	2,43	0,129	0,348
0,860	18,7	1,12	2 46	0,126	0,351
0,872	19,0	1,14	2,50	0,122	0,356
0,884	19,3	1,16	2,53	0,119	0,363
0,896	19,5	1,17	2,57	0,114	0,371
0,908	19,8	1,19	2,60	0,109	0,383
0,920	20,0	1,20	2,63	0,103	0,400
0,932	20,3	1,22	2,67	0,097	0,422
0,944	20,6	1,23	2,70	0,089	0,454

Figure 2 shows that the separation effect increases with the input speed, and the more so the higher the angular-momentum conservation factor, which causes the chamber diameter to increase. At the same time, the length also increases, since the axial speed increases. The relationships are linear. Further, the rate of increase in the chamber diameter itself increases with ε_W, whereas the length tends to fall. The latter is due to the features governing the tangential and axial components of the velocity.

As regards the adhesion to the wall, the proper design of the sprayer plays an important part, since this controls the droplet size and the spraying angle, in conjunction with the number and distribution of the sprayers. All of these factors are incorporated via the diameter and speed of a droplet at the boundary of the spraying zone, i.e., δ_0, $dr/d\tau \equiv v_{0p}$ and r_1.

Figure 3 shows the relationship of a chamber size to sprayer zone radius; these relationships and the conditions imposed on the initial velocities and droplet diameters indicate that spraying by a large number of jets providing a comparatively small spray divergence angle (about 45°) is necessary to provide for drying without deposition on the wall of the chamber.

We now consider how the dimensions of the drying chamber are affected by heat and mass transfer in the two-phase system as a whole; (14) shows that α_2 is dependent on the speed of the heat carrier, since increase in the latter accelerates the heat and mass transfer in the boundary layer and thus increases the rate of transfer between the droplets and the carrier.

The thermal conductivity of the gas has a similar effect on the heat-transfer rate; also, the thermal resistance of the boundary layer is reduced as the temperature is raised.

The heat-transfer factor is inversely proportional to the droplet diameter, but the bulk heat-transfer coefficient is inversely proportional to the square root of this $(1/\delta_{3.2}^{0.5})$ under the actual working conditions of a spiral sprayer chamber, so the accelerated heat transfer provided by reducing the droplet size is attained not only as a result of increasing the heat-transfer surface per unit weight, but also by increase in the heat-transfer coefficient.

In conclusion, we give an example of calculations on such a drying chamber with countercurrent spiral flows having a productivity of 300 liters/h (as evaporated water), the calculation being based on the parameters of an actual similar chamber of output 100 liters/h. By virtue of the symmetry, we consider only one half of the chamber. The geometrical parameters are $a = 0.07$ m; $k_a = 2$; $b = 0.175$ m; $a_{out} = 0.22$ m; $b_{out} = 0.22$ m; $R = 0.6$ m; $L = 2.1$ m, while the air flow rate is $Q = 1350$ kg/h, and the physical constants for $t_{av} = 120°C$ in the heat carrier are as follows: $\nu = 26.21 \cdot 10^{-6}\ m^2/sec$; $\gamma_1 = 0.87\ kg/m^3$; $\gamma_2 = 1000\ kg/m^3$; $\delta_0 = 10^{-4}$ m; $\delta_c = 10^{-5}$ m; $r_1 = 0.25$ m.

Solution of (7) and (10)-(13) gives

$$\tau_c = 0.226 \text{ sec}, \qquad \tau_x = 0.35 \text{ sec}, \qquad \varepsilon_w = 0.545.$$

We give the second stage in the calculation, in which the direct problem is solved. The physical setting in the chamber remains as before. To evaporate 150 liters/h requires 4500 kg/h of air. We specify ε_W = 0.6, ω = 10.0 sec^{-1} and vary r_1 in the range 0.5-0.9 to solve (7) and (10)-(13), which gives the results collected in Table 1. Then we use (14) to determine the chamber volume and we select the appropriate line of values from the table (line denoted by the bar).

The calculations thus incorporate the dynamics of individual droplets and also those of the two-phase system as a whole.

NOTATION

R, L, radius and length of the vortex chamber; a, b, k_a, height, width, and number of inlet pipes; a_{out}, b_{out}, height and width of outlet pipes; u, v, w, axial, radial, and tangential velocity components of heat carrier; ε_W, coefficient of angular-velocity conservation for the velocity near the wall; δ_0, δ_C, δ, $\delta_{3.2}$, initial, crust-formation, current, and mean volume-surface ratio diameters of drops; x, r, current coordinates; τ_C, τ, τ_X, crust-formation time, current time, and drying time, respectively; r_1, radius of spraying zone; w_{in}, w_{out}, heat-carrier velocities at the inlet and outlet, respectively; A_V, volume loading factor of chamber; $A_V = V_*/V_{ch}$, where V_* is the volume of solution evaporated in 1 h; V_{ch}, chamber volume; $Re_{(p)}$, $Re_{(in)}$, $Re_{(out)}$, Reynolds numbers based on particle, inlet, and outlet velocities, respectively, $Re_{(in)} = w_{in}k_a a/\nu$, $Re_{(out)} = w_{out}a_{out}/\nu$; m_p, mass of a particle; ψ, drag; s, area of midsection of a particle; γ_1, γ_2, densities of heat carrier and solution; q, acceleration; v, kinematic viscosity of heat carrier; λ, thermal conductivity of heat carrier at the mean temperature in the dryer. Indices: p, particle parameter.

LITERATURE CITED

1. A. V. Kalmykov, The Aerodynamics and Heat and Mass Transfer of Two-Phase Flows [in Russian], Nauka, Moscow (1970), p. 80.
2. L. S. Klyachko, Otoplenie i Ventilyatsiya, No. 4 (1934).
3. V. A. Fedoseev, Tr. Odessk. Gos. Univ. im. I. I. Mechnikov Ser. Fiz. Nauk, 50, No. 7, 27-327-32 (1960).
4. M. L. Lykov and B. I. Leonchik, Spray Dryers [in Russian], Mashinostroenie, Moscow (1966), p. 112.
5. O. A. Kremnev, V. R. Borovskii, and A. A. Dolinskii, High-Speed Drying [in Russian], Gostekhizdat, Kiev (1963).
6. G. N. Lance, Numerical Methods for High-Speed Computers [Russian translation], IL, Moscow (1962).